Optical second-harmonic generation by nanostructures: size effects and the role of quantum chaos

O. A. Aktsipetrov, P. V. Elyutin, A. A. Nikulin, and E. A. Ostrovskaya

M. V. Lomonosov Moscow State University, 119899 Moscow, Russia
(Submitted 28 July 1994)
Zh. Eksp. Teor. Fiz. **107**, 96–110 (January 1995)

We have studied second-harmonic generation in metallic nanocrystals and semiconductor quantum dots. Experimentally, the nonlinear response was found to be enhanced as the particle radius was reduced from some tens of nanometers to sizes of the order of a nanometer. A theoretical description based on noninteracting chaotically moving electrons within each particle is encouragingly consistent with the experimental data. © *1995 American Institute of Physics.*

1. INTRODUCTION

The unique physical properties of metallic nanocrystallites and semiconductor quantum dots have been widely studied in recent years. This is especially true of experimental observations and theoretical descriptions of the various size-induced quantization effects in such quasi-zero-dimensional systems,[1] which can be used as the structural components of modern composite materials and high-speed optoelectronic devices (such as optoelectronics switches, memory cells, etc.).

The spatial confinement of electron motion in metallic nanocrystallites and semiconductor quantum dots strongly influences both the linear and nonlinear properties of these systems. Enhanced optical nonlinearity in quantum dots (as compared with a bulk semiconductor sample) was predicted by Nakamura *et al.*[2] for the case in which there is significant size-induced quantization of exciton motion. Various third-order nonlinear optical effects have been investigated in semiconductor microcrystallites embedded in a glass matrix: degenerate four-wave mixing,[3] nonlinear absorption,[4] and coded second-harmonic generation.[5] Third-order (cubic) optical nonlinearity has been the preferred mode: experimental studies of cubic effects have been more convenient, given the assumption that quadratic effects like the generation of the reflected second harmonic should be negligible in macroscopic samples containing quantum dots and metallic nanocrystallites, and that those samples are centrosymmetric media (at the macroscopic level). The size dependence of the quadratic response of metallic and semiconductor nanostructures was first reported in Refs. 6 and 7.

Theoretical examination of the nonlinear optical response of small particles requires that one transcend the standard methods of solid-state theory. Particle shape and size take on special importance, since an appreciable fraction of the atoms in small particles are at the surface. Many theoretical models of small-particle optical response (in metallic nanocrystallites and quantum dots) presuppose a centrosymmetric shape (typically spherical).[9] A more realistic study of quadratic optical effects in small (nanometer-size) particles require allowance for variations in particle shape.

These variations, which are present in all mesoscale systems, cannot be discounted for at least two reasons. Firstly, the quadratic susceptibility of centrosymmetric systems vanishes in the dipole approximation. One might therefore expect that a small reshaping that breaks the inversion symmetry of the particles should lead to a sizable increase in second-harmonic optical response, due to the onset of a nonvanishing dipole contribution to the quadratic susceptibility. Secondly, a deviation from exact symmetry can destroy the integrability of electron motion. In the latter case, an electron in a small particle would have to be described by a quantum-chaotic system model. Its energy spectrum, the wave functions of stationary states, and the matrix elements of dynamical variables would then become random quantities subject to statistical description.[9,10] We would then be dealing with two fundamentally distinct sources of irregularity in the physical quantities. The first would be the mesoscale nature of the system, which is manifested in fluctuations of particle shape and other parameters characterizing the system. The second would be chaotic electron dynamics, which would show up no matter what the assumed shape of any particular particle, yielding electron motion that is no longer integrable.

Gor'kov and Eliashberg[11] modeled an electron in a small metallic particle using a completely random Hamiltonian belonging to a Gaussian ensemble. Subsequently, concurrently with the development of chaotic dynamics, Buch *et al.*[12] and Berry *et al.*[13] related the applicability of such a model to the size of the stochastic component at the energy surface of the system's classical analog. Although the relationship was established by analysis of two-dimensional systems (billiards and nonlinear oscillators), it was widely assumed to hold in three dimensions as well. To the best of our knowledge, however, there have thus far been no systematic studies of the nonlinear optical properties of metallic nanocrystallites and quantum dots based on quantum chaos theory. Specifically, there is as yet no faithful model with which to calculate the quadratic susceptibility of such systems.

In the present paper, we report an experimental and theoretical study of the quadratic optical response of metallic nanocrystallites and quantum dots as a function of mean particle size. In the experimental part of this study, we have relied on the generation of a reflected second harmonic. We lay special stress on the role played by the chaotic nature of electron motion in the theoretical interpretation of the size effects that we observed.

 1063-7761/95/010050-08$10.00

Our proposed model for calculating the small-particle response is based on two ideas. The first is that we assume the model matrix elements and energy-level separations to be random quantities with statistical properties dictated by the theory of strongly chaotic quantum systems. The second is that we invoke the correspondence principle to describe the smoothed behavior of these quantities, which are averaged over energy ranges that contain sufficiently many energy levels of the system. In particular, we replace the mean squared matrix elements of dynamical quantities with a specially normalized spectral density of their classical analogs.[14] In Sec. 4.2, we compare the size dependence of the quadratic susceptibility obtained in the quantum-chaotic model with that obtained via an alternative approach based on a model of regular electron motion.

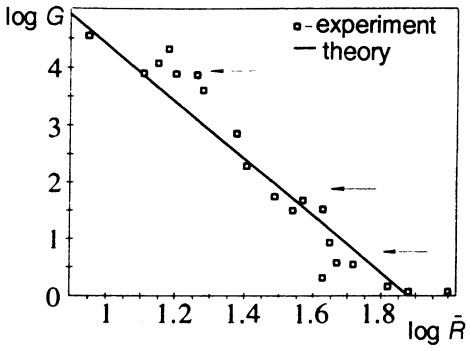

FIG. 1. Second-harmonic size-induced enhancement factor G as a function of mean radius $\bar{R}$ for silver particles ($\bar{R}$ in nanometers). Arrows indicate anomalies in the experimental size dependence.

2. EXPERIMENT

2.1. Metallic nanocrystallites

The size dependence of giant second-harmonic generation was studied in island films with ultrasmall particles (islands) of silver. Island-film samples were prepared by evaporating all elements in a high-vacuum chamber with a residual pressure of order 10^{-9} Torr. The substrate for the island film was a surface of NaCl monocrystals coated with a thin film of SiO. Prior to deposition, the NaCl monocrystals were heated to 700 K for surface cleaning. A 50-nm layer of SiO was then deposited, followed by the silver. The deposition rate was 2 nm sec^{-1}. Following deposition of the silver nanocrystallites, the films were coated with 50 nm of amorphous SiO to protect the metallic nanocrystallites from the influence of the ambient medium.

Following deposition, the resulting structures were separated into individual samples, which were subsequently investigated in nonlinear optics experiments and with a transmission electron microscope. Using a JEM 100 C electron microscope, we determined the following parameters of the island film: the mean particle radius $\bar{R}$, which ranged from 1 to 10 nm in our samples, the mass thickness d_m, which ranged from 0.1 to 3.4 nm, and the filling factor q, which ranged from 0.07 to 0.4. The characteristic particle radius was determined by averaging over an ensemble of several hundred islands.

We irradiated the island films with a Q-switched YAG:Nd^{3+} single-mode p-polarized laser (wavelength 1064 nm, pulse width 15 ns, repetition rate 12.5 Hz); the pump power density was $I_\omega \sim 0.5$ MW cm^2. No sample breakdown was observed at that intensity. Radiation at the frequency of the second harmonic was separated out with a double monochromator, and its intensity $I_{2\omega}$ was measured with a photomultiplier and a standard electronic sampling system. The detection system was calibrated in intensity using the reflected second harmonic signal for bulk samples of silver, which has the well-known value $I_{2\omega}/I_\infty^2 = 1.4 \cdot 10^{-27}$ in cgs units.[15]

Island-film samples differed from one another not only in terms of the mean radius $\bar{R}$ of islets, but in terms of the surface density $N^{(Ag)}$, and therefore the filling factor $q^{(Ag)} = \pi n^{(Ag)} \bar{R}^2$ varied from sample to sample. The measured value of the second harmonic intensity $I_{2\omega}$ cannot directly characterize the size effect in the quadratic optical response of the islands, since in our experiment $I_{2\omega}$ depended on two arguments, $\bar{R}$ and $q^{(Ag)}$ (or $\bar{R}$ and $n^{(Ag)}$). In order to isolate the unadulterated size effect, the measured intensity of the second harmonic was normalized via the procedure described in Sec. 2.3. The resulting size dependence is illustrated in Fig. 1.

2.2. Semiconductor quantum dots

In the present experiment, the second harmonic was generated by reflecting a 1064-nm YAG:Nd^{3+} laser beam from the surface of a composite material—a glass matrix with embedded crystallites of CdSe. Other details of the experiment have been described in Sec. 1.1.

The sample of semiconductor-doped glass was prepared by repeated annealing.[17] The density of CdSe by volume was approximately 0.5%, and the semiconductor content was uniform throughout the glass rod. Nanocrystallites in various parts of the glass rod ranged in size from 5 to 50 nm, which was achieved using a special secondary heating process. The monotonic progression of mean particle size along the experimental specimen was maintained by monitoring the absorption band edge.

The procedure employed to prepare the specimens that we studied thus ensured a constant filling factor

$$q^{(CdSe)} = \frac{4\pi}{3} n^{(CdSe)} \bar{R}^3,$$

where $n^{(CdSe)}$ is the bulk concentration of CdSe crystallites. In contrast to the situation in island films, this enabled us to treat the measured second-harmonic intensity solely as a function of $\bar{R}$ (see inset in Fig. 2). The experimental data normalized in accordance with the procedure described in Sec. 2.3 are shown in the main panel of Fig. 2.

2.3. Experimental data processing

The second-harmonic radiation was generated in these experiments by reflection from a macroscopically disordered two-dimensional (in the case of island films) or three-dimensional (in the case of CdSe crystallites in a glass ma-

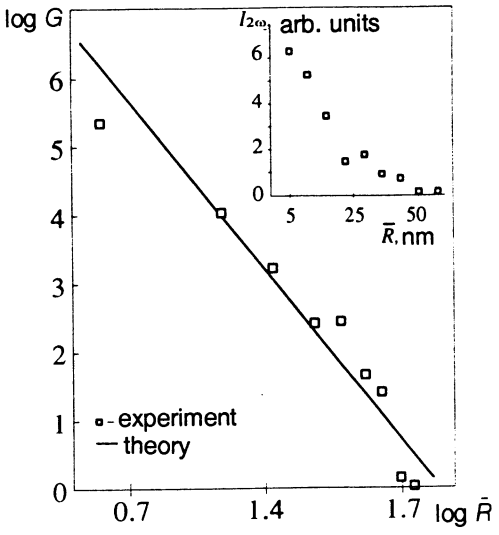

FIG. 2. Second-harmonic size-induced enhancement factor G as a function of mean radius $\bar{R}$ for CdSe crystallites ($\bar{R}$ in nanometers). The inset shows the intensity $I_{2\omega}$ of the second harmonic (arbitrary units) as a function of $\bar{R}$.

trix) array of particles. To identify the pure size effect in the quadratic response, it was necessary to derive an expression relating the intensity of the second harmonic to the effective quadratic susceptibility $\chi_2 \equiv \alpha_2/V$ of an individual particle (where α_2 and V are the quadratic polarizability and volume of a particle). More specifically, the particles can be considered dipoles oscillating at the frequency of the second harmonic, since the parameters of the systems treated here satisfy

$$\bar{R} \ll \bar{l} \ll \lambda_\omega, \tag{1}$$

where $\bar{R}$ is the mean particle radius, $\bar{l}$ is the mean distance between neighboring particles, and λ_ω is the pump wavelength. For silver islands $\bar{l}^{(\mathrm{Ag})} \propto (n^{(\mathrm{Ag})})^{-1/2}$, while for CdSe crystallites $\bar{l}^{(\mathrm{CdSe})} \propto (n^{(\mathrm{CdSe})})^{-1/3}$, where $n^{(\mathrm{Ag})}$ ($n^{(\mathrm{CdSe})}$) denotes the surface (bulk) particle density. The radiation detected at the second harmonic—from both the metal and semiconductor particles—was diffuse and depolarized, confirming the noisy nature of the nonlinear optical sources:

$$\overline{|\chi_2|^2} \gg |\overline{\chi_2}|^2, \tag{2}$$

where an overbar denotes averaging over the ensemble of particles. Taking (1) and (2) into consideration, we can write out an expression for the measured intensity of the diffuse component of the second harmonic generated by a disordered array of particles,

$$I_{2\omega}^{(\mathrm{exp})} \propto n \bar{V}^2 |L(2\omega,q) L^2(\omega,q)|^2 \overline{|\chi_2(\omega)|^2} I_\omega^2. \tag{3}$$

Here $n = n^{(\mathrm{Ag})}$, $n^{(\mathrm{CdSe})}$, $\bar{V}$ is the mean particle volume, I_ω is the pump intensity, and $L(\omega)$ and $L(2\omega)$ are local field factors that describe the mean corrections to the field introduced by the linear response of the environment of a particle at the pump and second harmonic frequencies. We assume that fluctuations in the local field factor and particle volume are negligible compared with fluctuations in the quadratic susceptibility. The local field factor depends on the local environment of the particles, and therefore turns out to be a function of the filling factor q ($q = q^{(\mathrm{Ag})}, q^{(\mathrm{CdSe})}$).

The function $\chi_2(\bar{R})$ can be defined in terms of the normalized intensity at the second harmonic:

$$\overline{|\chi_2(\bar{R})|^2} \propto I_{2\omega}^{(\mathrm{norm})}(\bar{R}) \equiv \frac{I_{2\omega}^{(\mathrm{exp})}(\bar{R})}{I_\omega^2 n \bar{V}^2 |L(2\omega,q^{(\mathrm{Ag})}) L^2(\omega,q)|^2}. \tag{4}$$

In order to express the denominator on the right-hand side of Eq. (4) as a known function of the measured parameters $\bar{R}$ and q, we have made several additional assumptions.

1. We assume that diversity in particle shape is small enough that it does not substantially affect $L(2\omega,q)$ or $\bar{V}$ (so that $\bar{V} = (4\pi\bar{R}^3/3)$. At the same time, such variations play a key role in the calculation of $\overline{|\chi_2|^2}$; see Sec. 3.

2. The linear optical response of a particle can be described with the aid of the local (bulk) dielectric constant: we assume that size-dependent nonlocal effects are negligible at experimentally achievable particle sizes (1 nm$\leqslant \bar{R}^{(\mathrm{Ag})} \leqslant$10 nm, 5 nm$\leqslant \bar{R}^{(\mathrm{CdSe})} \leqslant$50 nm).

3. $L(\omega,q)$ was calculated using the expression obtained in Ref. 16 in the effective-medium approximation.

Finally, the enhancement factor describing the size dependence of the quadratic optical response was taken to be

$$G(\bar{R}) \equiv I_{2\omega}^{(\mathrm{norm})}(\bar{R}) / I_{2\omega}^{(\mathrm{norm})}(\bar{R}_{\max}), \tag{5}$$

where $\bar{R}_{\max}^{(\mathrm{Ag})} \sim 10$ nm, $\bar{R}_{\max}^{(\mathrm{CdSe})} \sim 50$ nm.

We have plotted the experimental $G(\bar{R})$ data for silver islands in Fig. 1 and for CdSe crystallites in Fig. 2. It is clear that the quadratic response is enhanced by two orders of magnitude in metals and five orders of magnitude in semiconductor particles as particle size decreases.

3. THEORY

3.1. Model

We consider a particle to be a noninteracting set of electrons contained within an impenetrable quasispherical surface with mean radius $\bar{R}$. In what follows, we call this system a (three-dimensional) billiard. In treating interactions between the electrons and the crystal lattice, we will assume that the electrons obey the same dispersion relation as in bulk matter. Since we are dealing with intraband transitions in metallic particles and interband optical transitions in semiconductor particles with two different energy bands, for the electron mass m we must use the effective mass m_{eff} in the two cases. In a metallic particle, m_{eff} is the mass of a conduction electron, and in a semiconductor it has different values in the various energy bands.

Given the irregular shape of the billiard, we assume that the classical motion of the electrons, which are elastically reflected from the boundary, is completely ergodic over the energy surface. Accordingly, we will describe the quantum properties of the electron states in terms of the theory of random matrices.

Let E_n be an energy eigenvalue, and let λ_n be the typical linear extent of the region of space accessible to an electron of energy E_n. The system will be semiclassical if

$$\xi_n=\frac{\hbar}{\lambda_n\sqrt{2mE_n}}\ll 1, \tag{6}$$

for billiards, $\lambda_n\approx\bar{R}$. For metallic particles, we can assume that m is the free electron mass m_e, and that E_n is approximately equal to the Fermi energy E_F. For semiconductor particles, an E_n can be chosen in the range $0<E_n<2\hbar\omega-E_g$, where $\hbar\omega$ is the photon energy and E_g is the band gap.

Inserting numerical values, we can easily show that our model is manifestly semiclassical for metallic particles ($\xi_n\approx 10^{-2}$), and can be assumed to be semiclassical for semiconductor particles ($10^{-2}<\xi_n<1$). This justifies our subsequent use of the correspondence principle.

3.2. Quadratic susceptibility

By analogy with linear susceptibility, we can assume that the effective quadratic susceptibility of an electron in an external static potential equals the particle's total dipole moment per unit volume.

In the dipole approximation, the quantum-mechanical expression for a typical component $\chi_2\equiv\chi^{xxx}(2\omega)$ of the electron's effective quadratic susceptibility tensor in an external field that varies at frequency ω is[18]

$$\chi_2=\frac{e^3}{2\hbar^2}\sum_{nmk}\frac{x_{nm}x_{mk}x_{kn}}{(\omega_{mn}-2\omega-i\delta_{mn})(\omega_{kn}-\omega-i\delta_{kn})}. \tag{7}$$

Here n, m, and k denote electron eigenstates that belong to the discrete spectrum, the x_{ij} are matrix elements of the Cartesian coordinates between the various states, ω_{ij} is the corresponding transition frequency, and δ_{ij} is the relaxation constant. Summation over all electrons within the particle/billiard can be replaced by summation over states n of the individual electrons in (7). The matrix elements of the coordinates in (7) possess the same typical properties as matrix elements of dynamic quantities in a quantum chaotic system:[14] on an energy scale $[\rho(E)]^{-1}\ll\Delta E\ll E_n$, where $\rho(E_n)$ is the mean density of energy states, the matrix elements behave like statistically independent random variables. The off-diagonal matrix elements x_{ij} have a zero-mean Gaussian distribution.[14] The nonlinear susceptibility χ_2 of a chaotic system can therefore be considered a statistical variable.

A systematic statistical analysis of the quadratic susceptibility lies beyond the capabilities of existing theory. We will assume that fluctuations in the denominator of (7) are negligible by comparison with fluctuations in the numerator by virtue of the mutual repulsion of energy levels typical of chaotic systems.[9,10] This enables us to replace the denominator with a typical value. Assuming the spectral levels to be approximately equally spaced, we henceforth put $E_n\equiv\hbar\omega_n\approx\hbar n\omega_0$, where $\hbar\omega_0$ is the mean spacing between energy levels: $\hbar\omega_0\approx[\rho(E_n)]^{-1}$. This yields

$$\chi_2\sim\sum_n\frac{A_n}{\Delta_n^{(1)}\Delta_n^{(2)}}, \tag{8}$$

where

$$\Delta_n^{(1)}=(\omega_{mn}-2\omega-i\delta)\cong(n\omega_0+\Delta^{(1)}-i\delta),$$
$$\Delta_n^{(2)}=(\omega_{kn}-\omega-i\delta)\cong(n\omega_0+\Delta^{(2)}-i\delta), \tag{9}$$

and A_n is a combination of matrix elements:

$$A_n=\sum_{mk}x_{nm}x_{mk}x_{kn}. \tag{10}$$

The differences $\Delta^{(1)}$ and $\Delta^{(2)}$ are proportional to the spacing between levels: $\Delta^{(1),(2)}\approx\omega_0$. The relaxation constants in (9) are assumed equal: $\delta_{mn}\approx\delta_{kn}\equiv\delta$.

The statistical properties of (8) are now governed by the statistical properties of the numerator, i.e., by A_n. Given the statistical properties of x_{ij}, we have

$$\langle A_n\rangle=0.$$

From here on, angle brackets denote averaging over a spectral range ΔE that encompasses a large number of energy levels.

The reflected second harmonic intensity observed experimentally is dictated by σ_χ, the rms value of χ_2. Bearing in mind the Gaussian statistics of the matrix elements x_{ij}, we can express (8) in a form that includes only the two-point correlation function of the A_n:

$$\sigma_\chi^2\equiv\langle|\chi_2|^2\rangle\cong\sum_n\frac{\langle|A_n|^2\rangle}{(\Delta_n^{(1)})^2(\Delta_n^{(2)})^2}$$
$$+\sum_{nj}\frac{\langle|A_nA_{n+j}|\rangle}{(\Delta_n^{(1)}\Delta_{n+j}^{(1)})(\Delta_n^{(2)}\Delta_{n+j}^{(2)})}. \tag{11}$$

The second sum in (11) can be dropped for the following reason. In the semiclassical limit, the two-point correlation of matrix elements between adjacent levels can be replaced by the correlation of the Fourier amplitudes of the corresponding classical dynamic variables:

$$\langle x_{n,n'}x_{n+j,n'+j}\rangle|_{\hbar\to 0}\cong\langle x(\omega)x(\omega')\rangle. \tag{12}$$

Since classical stochastic motion in a billiard is a stationary random process, the Fourier components of the Cartesian coordinates under such motion is δ-correlated:[19]

$$\langle x(\omega)x(\omega')\rangle\cong S(\omega)\,\delta(\omega+\omega'), \tag{13}$$

where $S(\omega)$ is the spectral density of one of the coordinates. Two-point correlations such as $\langle|A_nA_{n+j}|\rangle$ are therefore negligible, and the second sum in (11) effectively vanishes.

We can thus estimate the typical nonlinear susceptibility in our model to be

$$\chi_2^t\equiv\sigma_\chi$$
$$\cong\frac{e^3}{2\hbar^2}\left[\sum_{nmk}\frac{\langle|x_{nm}|^2\rangle\langle|x_{mk}|^2\rangle\langle|x_{kn}|^2\rangle}{[(\omega_{mn}-\omega)^2+\delta^2][(\omega_{kn}-2\omega)^2+\delta^2]}\right]^{1/2} \tag{14}$$

In the semiclassical limit, we can estimate this quantity via the correspondence principle,[14] which makes it possible to express the mean squared matrix element in terms of the

spectral density $S(\omega)$ of the classical coordinate ($\omega_{ij}\equiv|E_i-E_j|/\hbar$) and the density $\rho(E)$ of the energy levels ($E\equiv(E_i+E_j)/2$):

$$\langle|x_{ij}|^2\rangle|_{\hbar\to 0}\cong\frac{S(\omega_{ij})}{2\pi\rho(E)}. \tag{15}$$

Assuming that the particles are approximately spherical, we can adopt for our model the spectral density obtained from the theory of stochastic motion in a quasicircular two-dimensional billiard.[20] The approximate expression for $S(\omega)$, which is good to about 10%, is then

$$S(\omega)\approx S_A(\omega)=20\bar{R}^2(\omega/\Omega)^6 \quad \text{for } \omega>2\Omega, \tag{16}$$

and $S(\omega)=0$ for $\omega<2\Omega$. The characteristic frequency is $\Omega=v/2\bar{R}$, where v is the electron velocity.

The density of states $\rho(E)$ for a metallic particle can be calculated directly:

$$\rho_{\rm M}(E)\cong\frac{V}{8\sqrt{2}\pi^2}\frac{m^{3/2}E^{1/2}}{\hbar^3}, \tag{17}$$

where $V\approx 4\pi\bar{R}^3/3$ is the volume of the billiard. A semiconductor particle can be reduced to an effectively "metallic" system by introducing the composite density of states[21]

$$\rho_{\rm c}(E)=\frac{2V}{(2\pi\hbar)^3}\int\delta(E_{\rm C}(\mathbf{p})-E_V(\mathbf{p})-2\hbar\omega)d\mathbf{p}, \tag{18}$$

where $E_{\rm C}(\mathbf{p})$ and $E_V(\mathbf{p})$ are the dispersion relations for the conduction and valence bands, and the electron reduced mass is

$$m_{\rm r}=m_{\rm C}m_{\rm V}/(m_{\rm C}+m_{\rm V}), \tag{19}$$

where $m_{\rm C}(m_{\rm V})$ is the electron effective mass in the conduction (valence) band.

3.3. Approximate parity

In a centrosymmetric system, the coordinate matrix element x_{ij} between states $|i\rangle$ and $|j\rangle$ of the same parity vanishes identically. Since at least one such element enters into each term in the sum (7), the quadratic susceptibility of a spherically symmetric particle vanishes as well. A small particle with a slightly deformed surface remains close to spherical in shape, but its central symmetry may be broken. We assume that all classical integrals of the motion are completely destroyed in an asymmetric particle, except for a parity-specific discrete integral of the motion with no classical analog (at least for an individual trajectory), which may be only weakly broken. By definition, the parity P_n of an eigenstate is

$$P_n=\int\Psi_n(\mathbf{r})\Psi_n(-\mathbf{r})d\mathbf{r}, \tag{20}$$

where $\Psi_n(\mathbf{r})$ is the wave function for the state $|n\rangle$ in the coordinate representation. The origin is chosen in (20) to be at the center of the sphere that approximates the particle. If the particle is only slightly asymmetric, we expect that $|P_n|\approx 1$. The sign of P_n can then be used to classify states as being "almost even" or "almost odd." Matrix elements x_{ij} between states with "almost the same" parity can differ from zero, and can be estimated to be

$$x_{ij}\cong\eta\tilde{x}, \tag{21}$$

where η is a dimensionless parameter that accounts for the extent to which the particle deviates from being centrosymmetric, while $\tilde{x}$ is a typical matrix element between states of "almost opposite" parity, and is given by the semiclassical asymptotic form (15).

The asymmetry coefficient η can be derived from addition considerations. Let the particle surface be given by $r=R(\varphi,\theta)$, where θ and φ are the azimuthal and polar angles of a spherical coordinate system. We shall assume that the function $R(\theta,\varphi)$ takes on random values. The deviation of a particle from sphericity is given by

$$\sigma_r^2=\frac{1}{\bar{R}^2}\overline{(R(\varphi,\theta)-\bar{r})^2}=\frac{1}{\bar{R}^2}\int(R(\varphi,\theta)-\bar{r})^2d\Omega, \tag{22}$$

where $\bar{r}\equiv\bar{R}$ and $d\Omega=\sin\theta\,d\theta d\varphi$. In an ensemble of randomly shaped particles, the deviations from sphericity will conform to some distribution. We that in mind, we define the asymmetry coefficient to be

$$\eta\approx\bar{\sigma}_{\rm r}, \tag{23}$$

where the overbar here represents an ensemble average, just as in Eq. (2) (see Sec. 2.3). The value of σ_r can be obtained from additional considerations.

An irregular but almost spherical surface can be modeled as a randomly deformed sphere[22]

$$R(\varphi,\theta)=\bar{R}(1+\varepsilon F(\varphi,\theta)), \tag{24}$$

where $\varepsilon\ll 1$ is the depth of modulation and $F(\varphi,\theta)$ is a random function with the following three properties.

1) $F(\varphi,\theta)$ can be expanded in essentially a finite number of spherical harmonics:

$$F(\varphi,\theta)=\sum_{l=N_{\rm L}}^{N_{\rm R}}\left\{\frac{1}{2}A_{l0}P_l(X)+\sum_{m=1}^{l}(A_{ml}\cos m\varphi+B_{ml}\sin m\varphi)P_l^m(X)\right\}$$

$$A_{ml}=C_{ml}\alpha_m,\quad B_{ml}=C_{ml}\beta_m,$$

$$C_{ml}=\sqrt{\left(\frac{2l+1}{2\pi}\right)\frac{(l-m)!}{(l+m)!}};\quad X=\cos\theta, \tag{25}$$

where the $P_l^m(X)$ are the associated Legendre functions.

2) $F(\varphi,\theta)$ is random: the coefficients α_n and β_n are random numbers with equal probability of taking the values 1, 0, and -1.

3) The objects we are studying are exceedingly small particles of crystalline matter. We can therefore use the lattice constant α_0 as the elementary deformation "step size" (or the minimum modulation amplitude). The effective harmonic l can then be defined as the ratio of the length of a deformed arc on the surface to the modulation amplitude:

$$l \approx \bar{R}/za_0, \tag{26}$$

where z is an integer; and

$$N_L \leqslant l \leqslant N_R,$$

$$\max N_R \equiv N_{max} \approx \bar{R}/a_0,$$

$$\min N_L \equiv N_{min} \approx 1. \tag{27}$$

The shape parameter, which defines the surface modulation amplitude in terms of the total number of harmonics $N=(N_R-N_L+1)^2$, is approximately

$$\varepsilon\sqrt{N} \approx a_0/\bar{R}. \tag{28}$$

Once the shape function $R(\varphi,\theta)$ has been defined, the degree of asymmetry η can be viewed as the degree of modulation, which can be characterized by the mean deviation from sphericity. A calculation of σ_r^2 using (22), with additional averaging over an ensemble of various deformations, yields

$$\eta \approx \left\langle \sigma_r \right\rangle_{ens} \approx \varepsilon\sqrt{N}\,\frac{[(N_R+1)^2-(N_L+1)^2]^{1/2}}{(N_R-N_L+1)^2}. \tag{29}$$

Thus, η depends on just two parameters that characterize the shape of the particle: the depth of modulation ε and the total number of harmonics N. Since these parameters are related to the particle size via (27) and (28), the asymmetry coefficient introduces an additional size dependence in the nonlinear susceptibility.

The information accessible about the details of particle shape[1] is not sufficient to directly determine ε, N, N_R, and N_L. We therefore choose plausible values for these quantities that are consistent with experimental measurements. Bearing in mind the possibility of subsequent experimental research, however, there are a number of considerations involved in the parametrization of particle shape in terms of N, N_R, and N_L.

1) The estimation of N, N_R, and N_L presupposes the feasibility of experimentally scanning the surface of an individual particle and subsequently tabulating the surface function $R(\theta,\varphi)$ (24) on a (θ,φ) coordinate grid. Using the data thus obtained, the surface of each particle in the experimental sample must be Fourier-analyzed to yield the dependence of the spectral density S_n^0 on the harmonic number n. The typical width Δ_n^0 of the spectrum S_n^0 then determines N_L, N_R, and $N=\Delta_n^0+1$ (a superscript 0 denotes quantities pertaining to an individual particle).

Note that $R(\theta,\varphi)$ reproduces the particle shape with no significant distortion only if the scanning step size is at most $\delta \sim a_0$, where a_0 is the lattice constant.

2) In an ensemble of particle shapes in an experimental sample, N_L, N_R, and N all conform to some distribution $P(\nu)(\nu \equiv N_L^0, N_R^0, N^0)$. Histograms of $P(\nu)$ enable one to determine N_L, N_R, and N from (27) and (28) (these we introduced for a "typical" particle in the sample) by finding the means of the corresponding distributions.

Note that the ensemble of particles must be large to provide the necessary raw data for the determination of $P(\nu)$ to sufficient accuracy. Specifically, if we assume that the individual realizations of particle shape are statistically independent, then to estimate N_L, N_R, and N on the basis of $P(\nu)$, we must process approximately 10^3spectra S_n^0 by the time we have $\nu \sim 10$.

3.4. Size dependence

The final expression for the nonlinear susceptibility, including the asymmetry coefficient, is

$$X_2^{type} \cong \frac{e^3}{2\hbar^2}\,\eta\left[\sum_{nmk} \bar{\chi}_{nmk}\right]^{1/2}, \tag{30}$$

where $\bar{\chi}_{nmk}$ is a typical term in the sum (14). The transition from a sum to an integral in this expression, which is possible in the semiclassical limit,

$$\sum_n \bar{\chi}_{nmk} \to \int \bar{\chi}_{nmk}\rho(E_n)dE_n, \tag{31}$$

enables one to obtain the scaling expression

$$\chi_2(2\omega) \approx K\eta\left(\frac{a_0}{\bar{R}}\right)^{1/2} \frac{a_{at}^3}{\mathscr{E}_{at}}\left(\frac{E_{at}}{\bar{E}}\right)^{7/4}, \tag{32}$$

where K is a numerical factor, and a_{at}, $\mathscr{E}_{at}$, and E_{at} are atomic units of length, electric field strength, and energy; $\bar{E}$ is the typical system energy.

The estimator (32) is based on the semiclassical expressions (15) and (16) for the matrix elements of a coordinate. The frequency scale in Eq. (16) for a metallic particle is set by the Fermi velocity: for a particle with radius $\bar{R} \cong 5$ nm we obtain $\Omega \cong 10^{14}$ sec^{-1}. For a semiconductor valence band, the frequency is of the same order of magnitude.

The characteristic energy $\bar{E}$ and the numerical coefficient K depend on the type of particle. For metallic nanocrystallites (silver in particular), $K \approx 3\cdot 10^{-5}$, and

$$\bar{E} \approx [(E_F+2\hbar\omega)(\hbar\omega)^3]^{2/7}E_F^{-1/7}. \tag{33}$$

For semiconductor (CdSe) quantum dots $K \approx 2\cdot 10^{-4}$; the characteristic energy $\bar{E}$ is dictated by the width of the band gap E_g and the photon energy $\hbar\omega$:

$$\bar{E} \approx [E_g(\hbar\omega)^3]^{2/7}(2\hbar\omega-E_g)^{-1/7}. \tag{34}$$

If $2\hbar\omega - E_g \to 0$, the energy $\bar{E}$ goes to infinity. In that event, our model can be viewed as being semiquantitative, since the requirement for semiclassical behavior is close to not being satisfied.

We note from (32) that the nonlinear susceptibility of an individual particle is a strong function of its size. The form of the dependence dictated by Eq. (32) can be compared with the experimental data.

4. RESULTS AND DISCUSSION

4.1. Size dependence of quadratic susceptibility

Figures 1 and 2, respectively, show the second-harmonic size-related enhancement factor G as a function of the radius of a metallic and semiconductor particle. In either case, it is proportional to the square of the susceptibility of an individual particle $[\chi_2]^2$ (see Sec. 2.3).

Depending on the specific irregularities in the particle surface, the theoretical formula (32) will yield a variety of size dependences. Surface modulation by a fairly large number N of harmonics with $N_{\min} \leqslant N \leqslant N_{\max}$ is the most plausible, both for metallic nanocrystallites and semiconductor particles, and it leads to a size dependence in the asymmetry coefficient

$$\eta \sim (a_0/\bar{R})^2. \tag{35}$$

Substituting (35) into (32), we obtain the susceptibility scaling law,

$$[\chi_2^t]^2 \sim (a_0/\bar{R})^5. \tag{36}$$

The corresponding theoretical plots for metallic nanocrystallites and semiconductor particles appear in Figs. 1 and 2.

4.2. Comparison with alternative theories

In the present work we have studied the effects of particle asymmetry on the quadratic optical response under the assumption that the perturbations in shape are large, so that the motion of electrons is completely nonintegrable. It must be stressed, however, that it is the breakdown of central symmetry rather than dynamical chaos *per se* that leads to the effects considered here.

A different limiting case, in which the changes in shape were small and electron motion remained entirely regular, was studied in Ref. 6. It was shown there that perturbations in particle shape can substantially affect the quadratic optical response of a particle consisting of a centrosymmetric substance (for example, Ag), since shape asymmetry results in a nonvanishing dipole contribution to the susceptibility. The presumed regularity of electron motion in this case enables one to use perturbation theory based on a coordinate-transformation method analogous to that employed in Ref. 22. This approach yields a somewhat weaker size dependence of the G factor for metallic nanocrystallites, $G \propto \overline{|\chi_2|^2} \sim \bar{R}^{-4}$. It would seem plausible that G should depend only weakly on the extent of electron dynamics regularity. But applying perturbation theory to the particles dealt with in this experiment (which have large $\bar{R}$ and a semiclassical energy spectrum) seems a bit too bold an extrapolation, capable of yielding only qualitative results.

The function $G(\bar{R})$ obtained in Ref. 7 is somewhat less consistent with the experimental data for island films than the size dependence given by Eq. (36). This discrepancy becomes more noticeable when one uses the correct normalization procedure, which takes account of the diffuseness of the second-harmonic radiation (see Sec. 2.3).

Equation (32) was derived in the nonresonant approximation, i.e., neglecting resonance effects associated with interband optical transitions in sufficiently small particles with a spatially quantized energy spectrum. It was shown in Ref. 7, however, that a resonance mechanism, in and of itself, can ensure that there will be an experimentally observable enhancement of the second harmonic in CdSe nanocrystallites, so more detailed study is necessary—both theoretical and experimental—of the relationship between resonant and nonresonant enhancement mechanisms in the optical response of crystallites with $\bar{R}^{(\mathrm{CdSe})} \sim 5$ nm.

Comparison with experiment shows that in either case (metallic nanocrystallites or semiconductor dots), the theoretical model employed here satisfactorily reproduces the basic trend in the behavior of the size dependence. For at least three reasons, however, one should not overestimate the agreement between theory and experiment.

First, certain of the experimental data cannot be reconciled with the present theoretical model, and may possibly suggest a more complicated nonmonotonic size dependence[23] (the corresponding experimental data points are indicated by arrows in Fig. 1).

Second, the paucity of experimental data on the details of particle shape makes this test of the theory incomplete, due to a substantial element of arbitrariness in the choice of shape parameters.

Third, in many respects the model studied here is a gross idealization. In our opinion, the most important physical factors still to be addressed are the following.

1) The lack of an explicit geometrical criterion for complete engodicity of motion in a three-dimensional billiard. What degree of surface irregularity ensures completely ergodic electron motion?

2) Electron interactions: how do they affect the randomness of electron motion? Conversely, how does stochastic motion modify multiparticle excitations such as surface plasmons, which are responsible for the resonant enhancement of the local field in metallic nanocrystallites?

3) Electron penetration beyond the surface due to the finite height of the confining potential. By describing the particle boundary as an infinitely high potential barrier, we have ruled this effect out. It was shown in Ref. 24, however, that the quadratic optical nonlinearity of metallic systems depends heavily on a self-consistent electron density profile in the boundary layer. We may thus question the sensitivity of our results to the shape of the boundary potential.

Every one of the foregoing questions deserves detailed and systematic study. Nevertheless, we suggest that the present work can serve as a starting point for further experimental and theoretical work, since our initial results in this domain demonstrate the importance of chaotic dynamics for a proper interpretation of nonlinear optical effects—and as might be expected, other physical phenomena—in solid-state nanostructures.

ACKNOWLEDGMENTS

We thank L. V. Keldysh, N. I. Koroteev, and O. Keller for fruitful discussions, and S. S. Elovinkov, N. N. Novikov, and A. I. Ekimov for providing the experimental samples. We are grateful to the *Solid-State Nanostructures, Low-Dimensionality Systems*; and *Precision Quantum Electronics* programs for their support. This work was supported by the International Scientific Foundation (Grant No. M12000), the Soros Foundation of the American Institute of Physics, and a grant from INTAS-93.

[1] H. Halperin, Rev. Mod. Phys. **58**, 533 (1986); C. Flytzanis, F. Hache, M.-C. Klein *et al.*, in Progress in Optics, E. Wolf (ed.), North-Holland, Amsterdam (1991).
[2] A. Nakamura, T. Tokizaki, H. Akiyama, and T. Kataoka, J. Luminesc. **53**, 105 (1992).
[3] H. Hosono, J. Abe, L. Lee *et al.*, Appl. Phys. Lett. **61**, 2747 (1992).
[4] S. Ohtsuka, T. Koyama, K. Tsunemoto *et al.*, Appl. Phys. Lett. **61**, 2953 (1992).
[5] N. M. Lawandy and R. L. MacDonald, J. Opt. Soc. Am. **B8**, 1307 (1991).
[6] O. A. Aktsipetrov, I. M. Baranova, E. M. Dubinina *et al.*, Phys. Lett. **A117**, 239 (1986).
[7] O. A. Aktsipetrov, A. I. Ekimov, and A. A. Nikulin, JETP Lett. **55**, 427 (1992).
[8] W. Ekardt, Phys. Rev. **B31**, 6360 (1985); F. Hache and D. Ricard, J. Phys. Condensed Matter **1**, 8035 (1989); O. Keller, in *Proc. First NATO Workshop on Nonlinear Optics*, Besançon, D. W. Pohl (ed.), Kluwer Academic, Dordrecht (1993).
[9] B. Eckhardt, Phys. Rep. **163**, 205 (1988).
[10] P. V. Elyutin, Usp. Fiz. Nauk **155**, 397 (1988) [Sov. Phys. Usp. **31**, 597 (1988)].
[11] L. P. Gor'kov and G. M. Eliashberg, Zh. Eksp. Teor. Fiz. **48**, 1407 (1965) [Sov. Phys. JETP **21**, 940 (1965)].
[12] V. Buch, R. B. Gerber, and M. A. Ratner, J. Chem. Phys. **76**, 5397 (1982).
[13] M. V. Berry and M. Robnik, J. Phys. Ser. A **17**, 2413 (1984).
[14] M. Feingold and A. Peres, Phys. Rev. **A34**, 591 (1986).
[15] N. Bloembergen, R. K. Chang, S. S. Jha, and C. H. Lee, Phys. Rev. **174**, 813 (1968).
[16] N. I. Koroteev and V. I. Emel'yanov, Usp. Fiz. Nauk **135**, 345 (1981) [Sov. Phys. Usp. **24**, 864 (1981)].
[17] A. I. Ekimov, A. Efros, and A. Onushchenko, Solid State Comm. **56**, 921 (1985).
[18] N. Bloembergen, *Nonlinear Optics*, Benjamin, New York (1965).
[19] L. D. Landau and E. M. Lifshitz, *Statistical Physics, Pt. 1*, 3rd ed., Pergamon, New York (1980), §122.
[20] P. V. Elyutin and E. A. Ostrovskaya, Dokl. Akad. Nauk **329**, 575 (1993) [Phys.-Dokl. **38**, 154 (1993)].
[21] V. L. Bonch-Bruevich and S. G. Kalashnikov, *Semiconductor Physics*, Nauka, Moscow (1990).
[22] K. F. Ratcliff, in *Multivariate Analysis V*, P. R. Krishnaiah (ed.), North-Holland, Amsterdam (1980), p. 593.
[23] O. Keller, M. Xiao, and S. Bozhevolnyi, Opt. Comm. **102**, 238 (1993).
[24] A. Liebsch and W. L. Schaich, Phys. Rev. **B40**, 5401 (1989).

Translated by Marc Damashek